Research Article

Prediction of specific hand movements using electroencephalographic signals

Cesar Marquez-Chin[1,2], Kathryn Atwell[1,2,3], Milos R Popovic[1,2,3]

[1]Rehabilitation Engineering Laboratory, Lyndhurst Centre, Toronto Rehabilitation Institute - University Health Network, Toronto, ON, Canada, [2]Therapeutic Applications of Complex Systems Laboratory, University Centre, Toronto Rehabilitation Institute - University Health Network, Toronto, ON, Canada, [3]Institute of Biomaterials and Biomedical Engineering, University of Toronto, Toronto, ON, Canada

Objective: To identify specific hand movements from electroencephalographic activity.
Design: Proof of concept study.
Setting: Rehabilitation hospital in Toronto, Canada.
Participants: Fifteen healthy individuals with no neurological conditions.
Intervention: Each individual performed six different hand movements, including four grasps commonly targeted during rehabilitation. All of them used their dominant hand and four of them repeated the experiment with their non-dominant hand. EEG was acquired from 8 different locations (C1, C2, C3, C4, CZ, F3, F4 and Fz). Time-frequency distributions (spectrogram) of the pre-movement EEG activity for each electrode were generated and each of the time-resolved spectral components (1 Hz to 50 Hz) was correlated with a hyperbolic tangent function to detect power decreases. The spectral components and time ranges with the largest correlation values were identified using a threshold. The resulting features were then used to implement a distance-based classifier.
Outcome measures: Accuracy of classification.
Results: A minimum of three different dominant hand movements were classified correctly with average accuracies between 65–75% across all 15 participants. Average accuracies between 67–85% for the same three movements were achieved across four of the 15 participants who were tested with their non-dominant hand.
Conclusion: The results suggest that it may be possible to predict specific hand movements from a small number of electroencephalographic electrodes. Further studies including members of the spinal cord injury community are necessary to verify the suitability of the proposed process.

Keywords: Brain-computer interfacing, Rehabilitation, Hand function, Electroencephalography, Spinal cord injury, Stroke

Introduction

Recent studies suggest that the use of a brain-computer interface (BCI) as part of a temporary therapeutic intervention to restore voluntary movement after spinal cord injury and stroke can result in greater and/or faster outcomes when compared to other interventions.[1–13] A BCI uses brain signals to control electronic devices. Although there are several approaches for implementing this technology, a common strategy consists of detecting changes in the activity of the brain related to motor activity. These changes, typically measured using standard electroencephalographic (EEG) techniques, are often observable not only during movement, but also before the actual movement starts and even by simply imagining it (i.e., no movement is actually required). This makes BCI technology suitable for operation by individuals with limited mobility as a potential access method. More importantly, the technology offers a unique opportunity to access neurological markers in real-time and integrate them into motor rehabilitation. For example, by using a BCI it could be possible to ensure that patients with high levels of impairment are engaged in motor tasks practiced during therapy or to facilitate an attempted movement by triggering suitable mechanism (e.g., electrical stimulation) at an optimal time to produce neuroplastic changes leading to motor recovery. It is believed that this increased precision afforded by BCI enhances the efficacy of therapy.

Correspondence to: Cesar Marquez-Chin, Therapeutic Applications of Complex Systems Laboratory, University Centre, Toronto Rehabilitation Institute - University Health Network, 550 University Avenue #12-104, Toronto, ON, M5G 2A2, Canada. Phone: (416) 597-3422 Ext.7899. Email: Cesar.Marquez@uhn.ca

DOI 10.1080/10790268.2017.1369215

The use of a BCI as a tool for restoring voluntary movement has taken two main approaches. First, patients can engage in BCI sessions in which they learn how to produce normal oscillatory EEG activity (e.g. power decreases in the mu and beta frequency ranges) by imagining movements of their impaired limbs. These sessions are immediately followed by regular physical therapy. Ramos-Murguialday *et al.*[1] recently reported the results of a study in which chronic stroke patients learned how to use a BCI by imagining movements of their impaired arm/hand. The BCI detected decreases in power of EEG in the mu and beta frequency ranges and activated an orthosis that would facilitate imagined movement. After a BCI session, patients would receive conventional physical therapy. The intervention resulted in significant changes in upper limb function. It is believed that the normalization of EEG activity leads also to the normalization of activity in any remaining neural structures involved in motor function resulting in an increased ability to move voluntarily.[3]

A second strategy for using a BCI as a short-term therapeutic intervention uses the technology to detect the patient's intention to move and simultaneously activate a device designed to produce the intended movement. In 2009, Daly *et al.* used functional electrical stimulation (FES) activated with a BCI to restore voluntary movements in a single participant 10 months after sustaining a stroke.[2] In the intervention the participant attempted to move her index finger and the BCI triggered an electrical stimulator to produce the intended movement. After nine sessions, the participant's ability to move her index finger voluntarily improved. Earlier this year, Donatti *et al.* presented a 12-month multi-stage intervention to restore gait combining BCI-activated lower limb actuators, visuo-tactile feedback, and an immersive virtual reality system.[14] The eight participants of that study had chronic (> 3 years) spinal cord injury (SCI) resulting in paraplegia and seven of them had complete injuries. Half of the participants' injuries were reclassified as incomplete at the end of the intervention with all of them showing improved somatosensory and motor control improvements. More recently, our group tested the efficacy of a BCI-triggered FES therapy to restore reaching movements in an individual with chronic severe hemiplegia resulting from a stroke sustained six years prior to the study. After 40 90-minute sessions (typical duration of our interventions), the participant registered a clinically meaningful improvement (Fugl-Meyer upper extremity sub score of 13 and 19 at the beginning and end of the intervention, respectively). Important to note is the fact that all other prior interventions, including FES alone, had failed to produce any change.[15]

The motivation for using a BCI to trigger an assistive device upon detection of a person's intention to move lies in the belief that matching the motor command (produced by an attempted movement) with its corresponding sensory feedback (generated by the artificially produced movement) produces changes in the central nervous system also resulting in improved motor function.[3] The same idea has also been proposed as an explanation for the recovery produced by FES,[16] for which we have developed technologies and interventions for two decades.[16–20]

At the moment, it is not known if identifying and facilitating specific movements, using a BCI in combination with other therapeutic interventions (e.g. FES therapy), will result in greater recovery of voluntary motor function. In addition to a precise indicator to inform when to facilitate an attempted movement, such a system would allow for the independent control of opposite movements (e.g. palmar grasp and hand opening) instead of a preprogrammed sequence of movements produced automatically, an approach commonly used today. This unprecedented level of transparency could, in turn, allow the inclusion of sequential movements initiated by patients in BCI-driven therapies

We present here a new approach toward predicting multiple hand movements performed with the same limb. This work represents an initial step towards testing the therapeutic effects of FES therapy that can identify and facilitate movements with a high degree of specificity.

Methods

Participants

Fifteen healthy adults participated in this study, approved by the Research Ethics Board of the Toronto Rehabilitation Institute University Health Network, after providing written informed consent (Table 1).

EEG Recordings

We recorded EEG from all participants over central and frontal regions (C1, C2, C3, C4, Cz, F3, F4, and Fz of the extended version of the 10–20 system for electrode placement), referenced to linked earlobes using the right clavicle as ground. The impedance was kept bellow 5 kΩ and we used a sampling frequency of 1 kHz (Synamps RT, Neuroscan, NC, U.S.A). EEG signals were high-pass filtered at 0.15 Hz prior to their recording.

Kinematic recordings

Participants wore a custom-made sensor glove, which captured the onset of hand movements using a resistive sensor (Fig. 1). The glove produced a variable

Table 1 Participant's demographics and completed tests

Participant	Age (Years)	Sex	Handedness	Completed test	
				Dominant hand	Non-Dominant hand
AA01	28	M	R	Yes	Yes
AA02	41	M	R	Yes	Yes
AA03	25	M	R	Yes	Yes
AA04	40	M	R	Yes	No
AA05	27	M	R	Yes	No
AA06	33	M	R	Yes	No
AA07	33	F	R	Yes	Yes
AA08	39	F	R	Yes	No
AA09	24	F	R	Yes	No
AA10	27	F	R	Yes	No
AA11	24	F	R	Yes	No
AA12	43	M	R	Yes	No
AA13	25	M	R	Yes	No
AA14	40	M	R	Yes	No
AA15	30	F	L	Yes	No

differential output (with a maximum amplitude of 5 mV) and was connected directly to the EEG headbox.

Additional Experimental Instrumentation

A photo resistor (optical sensor) detected the experimental cues provided to the participants on a computer monitor of each experimental trial. This sensor's differential output (maximum amplitude of 5 mV) was also connected to the EEG headbox. Figure 2 illustrates a normalized sample of the three types of recording: EEG, optical sensor, and sensor glove.

Procedure

Experimental Task

Participants performed six hand movements including: all-finger extension (hand opening), two-finger pinch, palmar grasp, lumbrical grasp and two tasks referred to as non-functional movements 1 and 2 (letters 'V' and 'Y' of the American Fingerspelled Alphabet, respectively) (Fig. 3). With the exception of the non-functional movements, all of the hand movements are commonly targeted during rehabilitation after stoke and spinal cord injury. All 15 participants completed the hand movements with their self-identified dominant hand and four of them repeated the experiment with their non-dominant hand during a second session, which was conducted to measure the robustness of the signal analysis developed for this study.

Experimental sequence

The participants were seated comfortably in front of a computer monitor throughout the duration of the experimental session. At the beginning of each trial, the participants were asked to relax for 10 seconds while focusing on a fixation cross. Next, visual cues were presented in the following sequence: a yellow circle (ready), a picture of the movement to execute, a green circle (go), and finally a red circle (stop). Each person completed six blocks of trials wherein the six hand movements were presented in a random order (Fig. 4). The participants were given the opportunity to rest between each block of trials.

Data Analysis

Feature Extraction

The EEG was processed offline with a custom-made Matlab ® (version 2012a, MathWorks, Natick, MA, U.S.A.) program. We first eliminated trials in which an incorrect movement or no movement was performed. Remaining trials were grouped according to the movement performed and aligned to the onset of movement determined with the output of the sensor glove. Seven

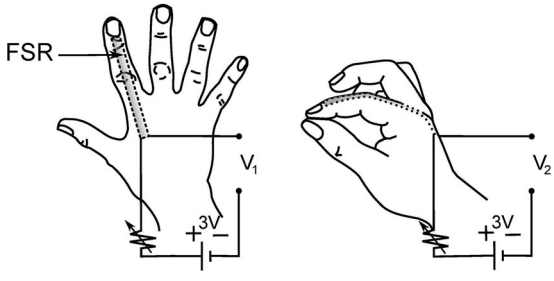

Figure 1 Illustration of sensor glove used to detect the onset of movement. A force sensitive-resistor was sewn into a glove overlaying the participant's first finger, indicated as FSR in Figure 1. The movement of the participants' hand creates a change in the FSR value (from 60–110kΩ) resulting in a change in voltage (Fig. 2).

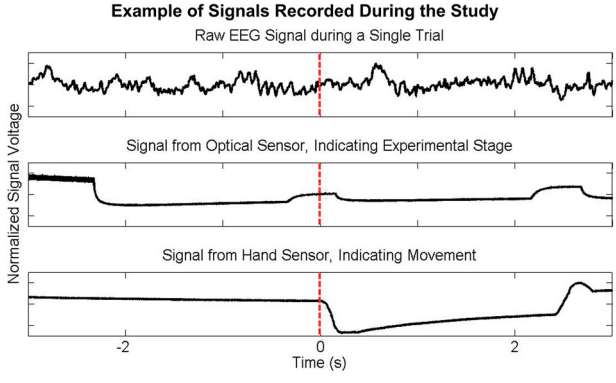

Figure 2 Example of signals recorded by the EEG amplifier during an experiment. Top row: an EEG signal from C3 location. Middle row: the output of the optical sensor placed against a monitor screen during the experiment, which was used to identify the stage (i.e. ready, go, stop) of the experiment. Bottom row: the output of a resistive sensor glove worn by participant during the experiment and was used to determine the onset of hand movement.

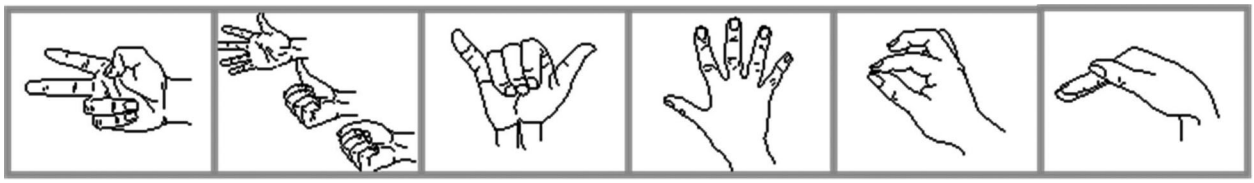

Figure 3 Illustration of the six hand movements performed by the participants. From left to right: non-functional grasp 1, palmar grasp, non-functional grasp 2, hand opening (extension of all fingers), two-finger pinch and lumbrical grasp. These movements were chosen based on their relevance to post-stroke rehabilitation (i.e. extension, two-finger pinch, lumbrical and palmar grasps). The two non-functional grasps were intended to provide additional test cases for the study.

seconds of each trial, including 4 s before and 3 s following the onset of movement, were extracted for further analysis. We performed a temporo-spectral decomposition of each trial using a 256-point Hamming window with a 120 sample overlap, and a resolution of 1 Hz for frequencies between 1 Hz and 50 Hz for each trial and electrode (*spectrogram* function, Matlab ®). This resulted in a 50×50 (time-frequency) matrix. Each time-resolved frequency component (1 Hz to 50 Hz) of every dataset was then normalized with respect to its own maximum value and smoothed using a moving average filter with a window length of 10 data points.

We then used a hyperbolic tangent function to approximate the general shape of a decrease of power (event related desynchronization or ERD[21]) typically observed prior and during voluntary movement:

$$ERD_{syn} = -(\tanh(4n)/3) + 0.5 \quad (1)$$

evaluated over 20 points with an intersample resolution of 0.1 (i.e., $n = [-0.8, -0.7, \ldots, 1.1]$. Next, we calculated the cross-correlation function between each of the time-resolved frequency components (which were 20 data points in length) and the hyperbolic tangent function (equation 1) at 20 instances prior to the onset of movement with an overlap between segments of 19 data points, over the period between 4 s and 0 s prior to the onset of movement. The correlation coefficients were estimated using the following equation:

$$\mathbf{R}(i, (ERD_{syn}, f_j)) = \frac{C(ERD_{syn}, f_j)}{\sqrt{C(ERD_{syn}, ERD_{syn})C(f_j, f_j)}} \quad (2)$$

where **R** refers to a matrix of cross correlation coefficients between the synthetic ERD signal (ERD_{syn}) and a time-resolved frequency signal (f_j), $j \in [1, 2, \ldots, 50]$ refers to each frequency analyzed, $i \in [1, 2, \ldots, 20]$ refers to each time instance the cross correlation calculation was applied. $C(ERD_{syn}, f_j)$ is the covariance between the ERD signal and a time-resolved frequency signal. $C(ERD_{syn,}ERD_{syn})$ is the variance of the ERD signal, and $C(f_j, f_j)$ is the variance of the time-resolved spectral component. Figure 5 shows the application of equation 2 for the first 16 time intervals.

A threshold n was then applied to the result of each sequence of cross-correlation calculations according to the following criterion:

$$\boldsymbol{G}(i, j, k)_n = \begin{cases} 1 & \boldsymbol{R}_{i,j} \geq n \\ 0 & \boldsymbol{R}_{i,j} < n \end{cases} \quad (3)$$

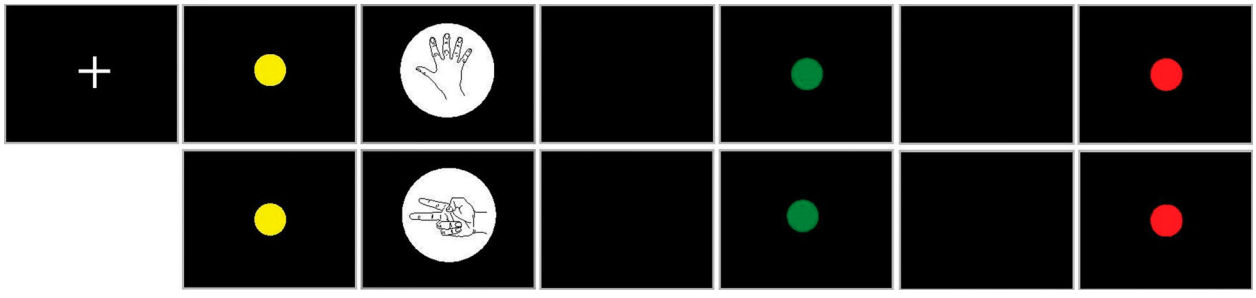

Figure 4 Sequence of scenes presented to the participant during a trial. Top row from left to right: 'fixation cross', presented to the participant at the start of every trial. A yellow circle, presented at time 1.0–3.5 s, indicating to the participant that a hand movement is about to be presented. A picture of the hand movement to be performed, presented at time 3.5–5.0 s. A black screen is then presented at time 5.0–7.0 s. A green circle, presented at time 7.0–7.5 s, indicating to the participant to perform the hand movement, followed by a black screen presented during the execution of the hand movement at time 7.5–9.5 s. Finally, a red circle, presented at time 9.5–10.0 s, indicating to the participant to relax their hand. Bottom row: The sequence is repeated with the next hand movement.

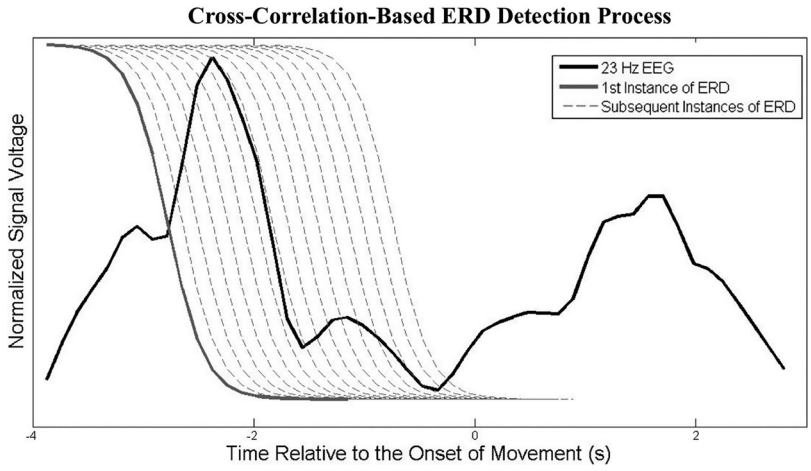

Figure 5 Illustration of the process by which cross-correlation coefficients were generated: In black, a 23 Hz smoothed and normalized time-resolved spectral component recorded during a two-finger pinch task. In grey, multiple instances of the synthetic ERD signal where cross-correlation coefficients were calculated. Movement onset occurred at 0s.

Where k is the number of trials available and $\boldsymbol{G}_n$contains binary values of correlations that exceed a specific threshold: $n \in [0.6, 0.65, 0.7, 0.75, 0.8, 0.85, 0.9]$.

For each hand movement and each electrode, an average (similar to the one presented in Fig. 6) was generated. We refer to these averages as 'all-in' templates because they include every trial in the averaged data set. For a single electrode site, each participant had six 'all-in' templates - one for each hand movement (Fig. 7). Next, 'one-out' templates were created by iteratively eliminating 1 trial and calculating the average of the remaining trials; for a hand movement executed 30 times, 29 'one-out' templates represented by 20×50×29 (time instances-frequency-trial number) three-dimensional arrays were generated.

Classification

The Euclidean distance between an 'all-in' template for a particular movement (Fig. 6) and an individual trial of a different hand movement was used as a measure of similarity between the two movements. For example, using data from a single electrode site and correlation threshold, the distance between the first trial of the non-functional movement 1 and the average of all trials of the two-finger pinch, was calculated with the

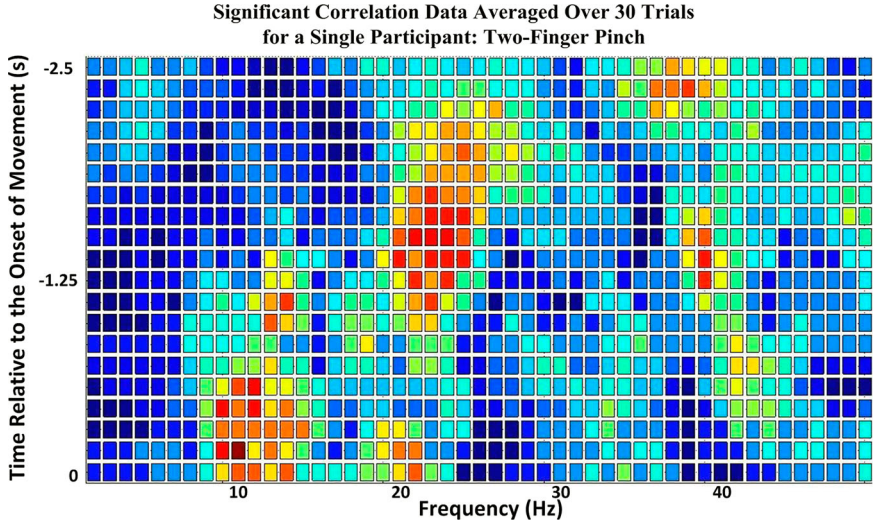

Figure 6 Example of the average of all significant correlation data for 30 trials of the two-finger pinch grasp ('all-in' template) for electrode F3 using a threshold of 0.8. The x-axis displays frequency from 1 to 50 Hz and the y-axis shows time intervals prior to the onset of movement. Warmer colours represent a higher instance of significantly correlated area.

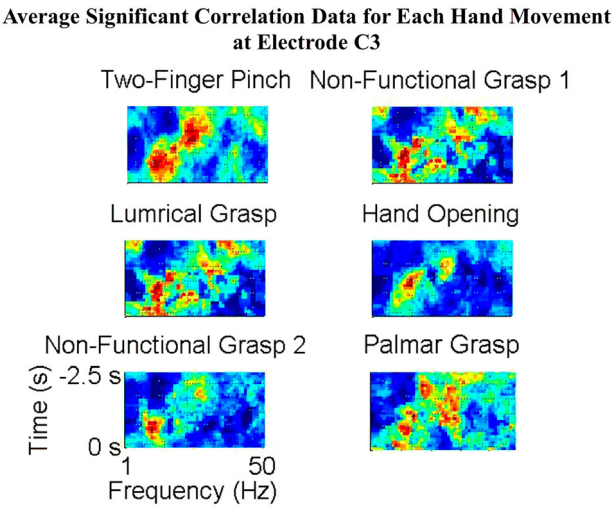

Figure 7 The average of all significant correlation data ('all-in' template) for each hand movement recorded with the C3 electrode. The x-axis displays frequency (1 Hz – 50 Hz) and the y-axis time intervals prior to the onset of movement. Warmer colours represent a higher incidence of significantly correlated area, and cooler colours represent a lower instance of significant correlations.

following equation:

$$\mathbf{D}(\Lambda i, \Lambda j)_{2,1} = \left| \mathbf{G}(i, j, 1) - \frac{\sum_{k=1}^{N_{Pinch}} \mathbf{G}(i, j, k)_1}{N_{Pinch}} \right| \quad (4)$$

Where $\mathbf{D}(\Lambda i, \Lambda j)_{2,1}$ is a matrix containing the element-to-element distances between the first trial of the non-functional movement 1 ($\mathbf{G}(i, j, 1)$) and the average of all trials of the two-finger pinch. For the rest of the classification process, equation 4 was then applied using the first trial of the non-functional movement 1 and the average of the remaining movements including the lumbrical grasp, hand opening, non-functional movement 2, palmar grasp, as well as the average of the non-functional movement 1. However, the average used for the non-functional 1 movement in this operation excluded the trial being classified.

The resulting six matrices containing the distances between trial 1 of non-functional movement 1 and all six movements were assembled in a 20×50×6 three-dimensional array. Next, this multi-dimensional array was summed along the 2nd dimension (i.e. frequencies included in the analysis), resulting in a 20×6 matrix. The minimum value at each time instance was then identified and assigned a value of 1 and all other entries given a value of 0. (Classification of an individual trial is possible through summation along the time dimension with the winning class identified by the largest result.) This process was then applied to every trial of non-functional movement 1, resulting in N_{NF1} 20×6 matrices, where N_{NF1} is the total number of non-functional 1 movement trials. The percentage of trials identified correctly as the non-functional 1 movement was then calculated.

To complete the classification for the non-functional movement 1, we repeated this process for every electrode site and every value of correlation threshold tested (listed above). The highest percentage of classification across 56 matrices (8 electrode sites×7 values for threshold) was selected to classify the movement. In addition, the time interval in which this value was found was indicative of the moment in which the classification had taken place, prior to the onset of movement. All of the movements were classified using the procedure described in this section.

In addition to estimating the classification accuracy using the information from all of the available electrodes, we explored the effects on the classification accuracy of the location of the electrodes included in the process (i.e. ipsilateral, contralateral, or placed along the midline), and of the hand (dominant or non-dominant) used to perform the movements.

Results

The participants performed between 141 and 187 trials. All of them completed the experiment using their dominant hand and four repeated the task with their non-dominant hand (Table 1).

Classification Accuracy

A minimum of three different dominant hand movements were classified with average accuracies greater than 60% across all 15 participants (Table 2). Average accuracies between 67–85% for the same movements were achieved across the four participants when tested with their non-dominant hand (Table 3). Among the hand movements included in this experiment, the palmar grasp was identified with the highest average accuracy (75.9% +/− 5.5%) and the lowest classification accuracy (2.4% +/− 0.7%) was obtained for the all-finger extension (hand opening) when results from all electrodes are averaged.

Effect of the Electrode Location on Classification Accuracy-Contralateral vs. Ipsilateral

There was a significant difference (t-test, $p=0.01$) between the averaged classification accuracies of the contralateral (53.0% +/− 14.4%) and ipsilateral (36.2% +/− 17.7%) electrode group for the non-

Table 2 Classification accuracies averaged across all participants, electrode groups, and correlation thresholds for dominant hand movements

Electrodes	Pinch % (±SD)	NF1 %(±SD)	Lumbrical %(±SD)	Extension %(±SD)	NF2 %(±SD)	Palmar %(±SD)
All	74.1(±4.1)	64.5(±11.7)	56.6(±15.8)	2.4(±0.7)	65.8(±10.0)	75.9(±5.5)
Contralateral	68.1(±4.6)	51.9(±17.2)	49.5(±16.2)	2.0(±0.8)	53.0(±14.4)	57.7(±15.6)
Ipsilateral	67.9(±6.6)	48.1(±18.7)	40.7(±18.2)	2.1(±0.7)	36.2(±17.7)	61.7(±13.4)
Vertex	65.5(±4.2)	50.1(±17.0)	34.1(±17.3)	1.0(±0.7)	43.1(±16.1)	62.2(±14.3)

functional movement 2 when performed with the dominant hand. No other significant difference in classification was found between the contralateral and ipsilateral electrodes. When the non-dominant hand was used, no significant differences between the contralateral and ipsilateral group were identified for any of the six movements (Tables 2 and 3).

Effect of Hand Dominance on Classification Accuracy

There was one statistically significant difference in classification between the dominant (66.5%) and non-dominant (44.8%) hand (t-test, $p=0.04$): the pinch grasp was classified with a significantly higher average accuracy when the dominant hand was used for the Cz and Fz electrode group (Fig. 8).

Classification prior to Movement Onset

The average time when each trial was successfully classified ranged from: 1.2 s +/− 0.8 s to 0.7 s +/− 0.9 s prior to movement for the dominant hand, and 0.7 s +/− 0.9 s to 0.4 s +/− 0.4 s for non-dominant hand movements across participants (Table 4).

Discussion

This report, to the best of our knowledge, is the first on the prediction of different hand movements targeted in rehabilitation of stroke and spinal cord injuries using EEG activity. The method described here is able to differentiate a minimum of three different movements from pre-motor EEG activity for every participant enrolled in this study, with individual accuracies between 60–100% and average accuracies between 67% and 85%.

The focus of our work was the development of a simple feature extraction process and we will explore more sophisticated techniques in our future work. Our results are similar to the results reported by Zhou *et al.*[22] (92% accuracy for prediction of elbow flexion and shoulder abduction torque) and Xiao[23] (45% for individual finger decoding). However, our work presented here used a maximum of eight EEG electrodes, compared to the 163[22] and 128 sensors,[23] making it more viable for its use in a clinical setting.

Not surprisingly, our results suggest that the relationship between the type of movement performed and location of relevant EEG features cannot be generalized across the participants included in this study. It is important to mention that we have not tested the presented method using data collected across multiple days. Investigation on the stability of the method across different recording sessions, as well as other elements such as fatigue, are warranted.

The EEG event of interest to the proposed method (ERD) has been observed as early as 1.5 s prior to movement, and was detected in a recent study in real-time an average of 0.62 s before movement.[24] The average time intervals reported using the proposed classification method are within this range. However, the inter-trial variance associated with the reported average for the same movement for each participant suggest that the time in which the ERD takes place is unique to the individual, the movement, and the trial.

Classification of hand opening movements was unsuccessful (< 16%) in all participants. Predictably, when all data pertaining to hand opening were removed post-hoc, the average accuracy of movement

Table 3 Classification accuracies averaged across all participants, electrode groups, and correlation thresholds for non-dominant hand movements

Electrodes	Pinch %(±SD)	NF1 %(±SD)	Lumbrical %(±SD)	Extension %(±SD)	NF2 %(±SD)	Palmar %(±SD)
All	67.5(±4.2)	78.7(±9.5)	76.0(±9.8)	2.6(±0.08)	62.3(±6.1)	85.1(±5.2)
Contralateral	63.6(±3.0)	73.0(±9.6)	56.8(±21.2)	2.0(±0.6)	41.8(±14.0)	83.2(±5.1)
Ipsilateral	53.8(±17.9)	54.5(±19.6)	69.3(±6.5)	1.1(±0.6)	46.8(±16.9)	76.0(±6.9)
Vertex	59.8(±5.8)	80.3(±7.3)	75.9(±6.5)	2.4(±0.04)	35.3(±15.4)	83.2(±4.0)

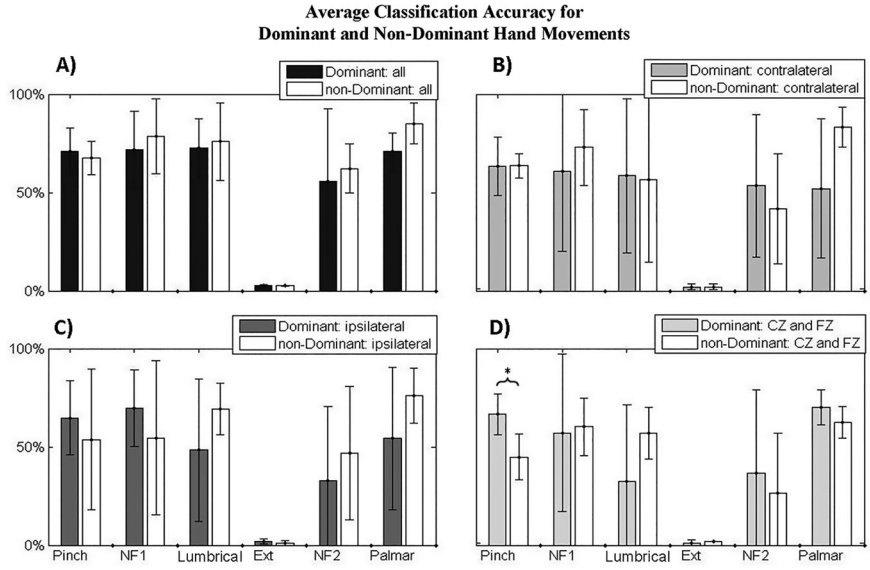

Figure 8 Average classification accuracy for dominant vs. non-dominant hand movements, for each electrode group. Graph A: all electrodes were used, graph B: only contralateral electrodes were used, graph C: only ipsilateral electrodes were used, and graph D: only CZ and FZ electrodes were used. Error bars refer to the standard deviation of each average value

classification improved significantly when the dominant hand was used (Table 5). Inspection of the hand opening data that were identified incorrectly revealed that the majority of these trials were classified as a non-functional movement 2 (44%) or palmar grasp (31%) (Table 6). None of the hand extension trials were confused with the pinch grasp and very few were identified incorrectly as the lateral pinch (2.3%).

Speculatively, the activity of motor planning related to all-finger extension may be similar to that required for the non-functional movement 2 or palmar grasp due to their similarity in the initial posture prior to hand shaping (i.e. for non-functional 2 or palmar grasp that hand had to be in finger extension posture first to assume the desired grasping posture, which is not necessarily the case with the three remaining grasps). All-finger extension requires the full extension of the thumb, which is also required for the non-functional movement 2, and the palmar grasp is performed from an initial position of finger extension. In contrast, the pinch grasp requires thumb flexion. The ubiquitous nature of finger extension may allow it to be classified as other hand movements, which also require thumb extension. However, the results of this study are insufficient to verify this observation.

With respect to the use of correlation for detecting ERD events, it is a method that has been used for detection of visual evoked potentials[25,26] and, as mentioned previously, to identify movements from different parts of the body. Inspection of Figure 6 reveals that the frequencies that are most strongly correlated with the hyperbolic tangent function fall within the mu (9Hz–13 Hz) and beta (19–25 Hz) ranges, which is in agreement with extensive literature. Additionally, the decrease in power visible in Figure 5 for a spectral component of 23 Hz observed during a single trial of two finger pinch takes place at approximately 1.7 seconds prior to the onset of movement, as predicted by Figure 6. In addition, it is unlikely that the spectral interpolation used in the work affected the classification results significantly.

Although the results presented here were obtained with participants without neurological conditions, the fact that the movement classification could be performed using information prior to the onset of movement exclusively suggests that it may be possible to apply the presented work to recordings obtained from persons with paralysis, including individuals with spinal cord injury. Indeed, the method presented here

Table 4 Average time prior to movement during which classification takes place for dominant hand movements

	Pinch s(±SD)	NF1 s(±SD)	Lumbrical s(±SD)	Extension s(±SD)	NF2 s(±SD)	Palmar s(±SD)
Dominant	–0.8(±0.7)	–0.9(±0.7)	–0.7(±0.9)	–0.8(±0.8)	–1.0(±0.9)	–1.2(±0.8)
Non-Dominant	–0.4(±0.4)	–0.6(±0.5)	–0.4(±0.7)	–0.5(±0.4)	–0.6(±1.0)	–0.7(±0.9)

Table 5. Average values and standard deviation of dominant hand classifications of movement using each electrode group with hand extension was either excluded or included in the experimental data

Electrode Set	Pinch	Pinch (without)	NF1	NF1 (without)	Lateral	Lateral (without)	NF2	NF2 (without)	Palmar	Palmar (without)
	%	%	%	%	%	%	%	%	%	%
All	74.1	82.4	64.5	82.8	56.6	81	65.8	81.6	75.9	83.6
+/− SD	(8.36)	(6.03)	(23.5)	(9.29)	(31.6)	(10.3)	(20)	(9.29)	11	(5.76)
Contralateral	68.1	76.9	51.9	78.9	49.5	69.8	53	70	57.7	71.8
+/− SD	(9.24)	(9.51)	(34.5)	(12.1)	(32.4)	(21.7)	(28.9)	(22.2)	(31.1)	(22.5)
Ipsilateral	67.9	76.9	48.1	71.9	40.7	71.2	36.2	69.2	61.7	72.7
+/− SD	(13.3)	(8.27)	(37.3)	(23.2)	(36.4)	(22.5)	(35.5)	(30)	(26.7)	(21.6)
CZ and FZ	65.5%	69.2	50.1	72.6	34.1	66.9	43.1	69.6	62.2	77.3
+/− SD	(8.46)	(20.4)	(34. 1)	(12.4)	(34.6)	(21.5)	(32.1)	(12.2)	(28.6)	(5.71)

should be tested with neurological populations. It is likely that the techniques will require modifications to accommodate the changes observed after the voluntary motor function is affected (e.g., cortical changes and a potential change of handedness).

Conclusion

The method described here is able to classify at least three of the six hand movements measured for every participant enrolled in this study with accuracies between 65% and 85% using either the dominant or non-dominant hand. Furthermore, since the EEG data used for movement classification was limited to only pre-motor activity, the proposed method is able to both differentiate and predict the hand movement that will be performed with reasonable accuracy. Accordingly, our results suggest that different hand movements are correlated to distinct features of the EEG.

The averaged classification accuracy for this group of participants did not change significantly when the electrodes used were limited to either the contralateral, ipsilateral, or CZ and FZ electrodes during dominant hand movements. Individually, however, the results reveal a spatial pattern of electrodes unique to both the individual and the movement performed. Therefore, if this system were to be implemented using the least possible number of electrodes, an initial study to evaluate the effectiveness of each electrode group in classifying the desired hand movement would be required.

Four of the 15 participants repeated the experiment using their non-dominant hand; a comparison between the results of both experiments revealed no significant difference in the average classification accuracy of the movements when performed with either the dominant or non-dominant hand. However, the small sample size for the non-dominant hand experiment makes it difficult to draw any relevant conclusion regarding the proposed methods ability to classify non-dominant hand movements. Additional studies in which more participants complete both the dominant and non-dominant hand experiments multiple times across several sessions are warranted.

The results of this study should be viewed as an exploratory report of potential EEG features effective for classification of specific hand movements towards the development of an online movement classification method. They will provide initial boundaries for this challenge and hopefully facilitate the development of a BCI able to detect different intended hand grasps in real-time for motor rehabilitation applications.

Table 6 Percentage of incorrect classifications of finger extension (hand opening) classified as one of the remaining five hand movements

	Pinch	NF1	Lateral	Extension	NF2	Palmar
Incorrect classification of finger extension	0%	22%	2.3%	0%	44.1%	31.4%

Declaration of Interests

The authors report no declaration of interest.

Acknowledgements

We would like to thank Mr. Aaron Marquis and Ms. Vanessa Zoras for their assistance. This work was supported by the Natural Science and Engineering Research Council of Canada [249669]; the Government of Ontario; the Dana Foundation; and the Dean Connor and Maris Uffelmann Donation.

Disclaimer statements

Contributors None.

Funding None.

Declaration of interest: None.

Conflicts of interest None.

Ethics approval None.

References

1 Ramos Murguialday A, Broetz D, Rea M, Läer L, Yilmaz Ö, Brasil FL, *et al.* Brain–machine interface in chronic stroke rehabilitation: A controlled study. Ann Neurol. Wiley Online Library; 2013;74(1):100–8.

2 Daly JJ, Cheng R, Rogers J, Litinas K, Hrovat K, Dohring M. Feasibility of a New Application of Noninvasive Brain Computer Interface (BCI): A Case Study of Training for Recovery of Volitional Motor Control After Stroke. J Neurol Phys Ther. 2009;33(4):203–11.

3 Daly JJ, Wolpaw JR. Brain–computer interfaces in neurological rehabilitation. The Lancet Neurology. 2008;7(11):1032–43.

4 Dobkin BH. Brain-computer interface technology as a tool to augment plasticity and outcomes for neurological rehabilitation. J Physiol. 2007;579(Pt 3):637–42.

5 López-Larraz E, Trincado-Alonso F, Rajasekaran V, Pérez-Nombela S, del-Ama AJ, Aranda J, *et al.* Control of an Ambulatory Exoskeleton with a Brain–Machine Interface for Spinal Cord Injury Gait Rehabilitation. Front Neurosci. Frontiers; 2016;10(122):e103764.

6 Liu Y, Li M, Zhang H, Wang H, Li J, Jia J, *et al.* A tensor-based scheme for stroke patients' motor imagery EEG analysis in BCI-FES rehabilitation training. J Neurosci Meth 2014;222:238–49.

7 Caria A, Weber C, Brötz D, Ramos A, Ticini LF, Gharabaghi A, *et al.* Chronic stroke recovery after combined BCI training and physiotherapy: a case report. Psychophysiology. 2011;48(4):578–82.

8 Rohm M, Schneiders M, Müller C, Kreilinger A, Kaiser V, Müller-Putz GR, Rupp R. Hybrid brain–computer interfaces and hybrid neuroprostheses for restoration of upper limb functions in individuals with high-level spinal cord injury. Artif Intell Med. 2013;59(2):133–42.

9 Ethier C, Miller LE. Brain-controlled muscle stimulation for the restoration of motor function. Neurobiol Dis. 2015;83:180–90.

10 Pichiorri F, Morone G, Petti M, Toppi J, Pisotta I, Molinari M, *et al.* Brain-computer interface boosts motor imagery practice during stroke recovery. Ann Neurol. 2015;77(5):851–65.

11 Nagaoka T, Sakatani K, Awano T, Yokose N, Hoshino T, Murata Y, *et al.* Development of a new rehabilitation system based on a brain-computer interface using near-infrared spectroscopy. Adv Exp Med Biol. 2010;662:497–503. In: Takahashi E., Bruley D. (eds) Oxygen Transport to Tissue XXXI. Adv Exp Med Biol. 662.

12 Prasad G, Herman P, Coyle D, McDonough S, Crosbie J. Applying a brain-computer interface to support motor imagery practice in people with stroke for upper limb recovery: a feasibility study. J Neuroeng Rehabil. 2010;7:60.

13 King CE, Wang PT, McCrimmon CM, Chou CC, Do AH, Nenadic Z. The feasibility of a brain-computer interface functional electrical stimulation system for the restoration of overground walking after paraplegia. J Neuroeng Rehabil. 2015;12(1):80.

14 Donati ARC, Shokur S, Morya E, Campos DSF, Moioli RC, Gitti CM, *et al.* Long-Term Training with a Brain-Machine Interface-Based Gait Protocol Induces Partial Neurological Recovery in Paraplegic Patients. Sci Rep. 2016;6:30383.

15 Marquez-Chin C, Marquis A, Popovic MR. EEG-Triggered Functional Electrical Stimulation Therapy for Restoring Upper Limb Function in Chronic Stroke with Severe Hemiplegia. Case Rep in Neurol Med. 2016;2016: Article ID 9146213.

16 Popovic MR, Kapadia N, Zivanovic V, Furlan JC, Craven BC, McGillivray C. Functional electrical stimulation therapy of voluntary grasping versus only conventional rehabilitation for patients with subacute incomplete tetraplegia: a randomized clinical trial. Neurorehabil Neural Re. 2011;25(5):433–42.

17 Kapadia NM, Nagai MK, Zivanovic V, Bernstein J, Woodhouse J, Rumney P, *et al.* Functional Electrical Stimulation Therapy for Recovery of Reaching and Grasping in Severe Chronic Pediatric Stroke Patients. J Child Neurol. 2014;29(4):493–9.

18 Kapadia NM, Zivanovic V, Furlan JC, Craven BC, McGillivray C, Popovic MR. Functional electrical stimulation therapy for grasping in traumatic incomplete spinal cord injury: randomized control trial. Artif Organs. 2011;35(3):212–6.

19 Popovic MR, Keller T. Modular transcutaneous functional electrical stimulation system. Med Eng Phys. 2005;27(1):81–92.

20 Popovic MR, Thrasher TA, Zivanovic V, Takaki J, Hajek V. Neuroprosthesis for retraining reaching and grasping functions in severe hemiplegic patients. Neuromodulation. 2005;8(1):58–72.

21 Pfurtscheller G, Aranibar A. Evaluation of event-related desynchronization (ERD) preceding and following voluntary self-paced movement. Electroen Clin Neuro. 1979;46(2):138–46.

22 Zhou J, Yao J, Deng J, Dewald JPA. EEG-based classification for elbow versus shoulder torque intentions involving stroke subjects. Comp Biol Med. 2009;39(5):443–52.

23 Xiao R, Ding L. Evaluation of EEG Features in Decoding Individual Finger Movements from One Hand. Comput Math Methods Med. Hindawi Publishing Corporation; 2013;2013: Article ID 243257.

24 Bai O, Rathi V, Lin P, Huang D, Battapady H, Fei D-Y, *et al.* Prediction of human voluntary movement before it occurs. Clin Neurophysiol. 2011;122(2):364–72.

25 Cilliers PJ, Van Der Kouwe AJW. A VEP-based computer interface for C2-Quadriplegics. Proc IEEE Eng Med Biol. 1993;15(Pt 3): 1263–4.

26 Sutter EE. The brain response interface: communication through visually-induced electrical brain responses. J Microcomput Appl. 1992;15(1):31–45.